

Measurement of $d+{}^7\text{Be}$ cross sections for Big-Bang nucleosynthesis

N. Rijal,¹ I. Wiedenhöver,¹ J.C. Blackmon,² M. Anastasiou,¹ L.T. Baby,¹

D.D. Caussyn,¹ P. Höflich,¹ K.W. Kemper,¹ E. Koshchiy,³ and G.V. Rogachev^{4,3}

¹*Physics Department, Florida State University, Tallahassee, FL 32306**

²*Department of Physics and Astronomy, Louisiana State University, Baton Rouge, LA 70803*

³*Cyclotron Institute, Texas A&M University, College Station, TX 77843*

⁴*Department of Physics & Astronomy, Texas A&M University, College Station, TX 77843*

(Dated: December 13, 2018)

The cross sections of nuclear reactions between the radioisotope ${}^7\text{Be}$ and deuterium, a possible mechanism of reducing the production of mass-7 nuclides in Big-Bang nucleosynthesis, were measured at center-of-mass energies between 0.2 MeV and 1.5 MeV. The measured cross sections are dominated by the (d, α) reaction channel, towards which prior experiments were mostly insensitive. A new resonance at 0.36(5) MeV with a strength of $\omega\gamma = 1.7(5)$ keV was observed inside the relevant Gamow window. Calculations of nucleosynthesis outcomes based on the experimental cross section show that the resonance reduces the predicted abundance of primordial ${}^7\text{Li}$, but not sufficiently to solve the primordial lithium problem.

Soon after the discovery of the cosmic microwave background in 1965 [1, 2], the primordial elemental composition of the universe was used as supporting evidence for the Big-Bang hypothesis and a means to determine cosmological parameters [3]. The major parameters of cosmology have now been precisely constrained, primarily by observations of the cosmic microwave background with COBE, WMAP and Planck [4–6]. The most important parameter for Big Bang nucleosynthesis (BBN) is the baryon-to-photon ratio, now determined to be $\eta = 6.079(9) \cdot 10^{-10}$ [6], allowing essentially parameter-free predictions for the primordial isotopic mass fractions under standard assumptions. The predicted mass fractions from BBN agree very well with the observations for ${}^2\text{H}$, ${}^3\text{He}$ and ${}^4\text{He}$. In sharp contrast, the value observed for ${}^7\text{Li}$, $(\text{Li}/\text{H})_P = 1.58_{-0.2}^{+0.35} \cdot 10^{-10}$ [7], is lower by a factor of 3-4 from the value calculated for Big-Bang nucleosynthesis (BBN).

This discrepancy, the “primordial lithium problem”, has been studied in multiple works, e.g. [8–10]. Possible solutions include the destruction of mass-7 nuclides through interactions with WIMP particles or non-standard cosmologies (Ref. [8] and references within). Other proposals assume the existence of ${}^8\text{Be}$ as a bound nuclide during BBN, based on an assumed variation of natural constants [11, 12]. These interpretations assume that the relevant nuclear reaction rates are known accurately.

In the conditions of BBN, ${}^7\text{Li}$ is effectively destroyed through ${}^7\text{Li}(p, \alpha){}^4\text{He}$, to a level that the majority of the surviving ${}^7\text{Li}$ is produced indirectly through the decay of the ($T_{1/2} = 53.12d$) radioisotope ${}^7\text{Be}$ after the cessation of nucleosynthesis. The most important nuclear aspects of the ${}^7\text{Li}$ problem are therefore the reaction rates of ${}^7\text{Be}$ production, mainly ${}^4\text{He}({}^3\text{He}, \gamma){}^7\text{Be}$, and its destruction through the reactions ${}^7\text{Be}(n, p){}^7\text{Li}$, ${}^7\text{Be}(n, \alpha){}^4\text{He}$ and $d+{}^7\text{Be} \rightarrow p+2\alpha$, specifically at temperatures around 0.8 GK [9, 10]. The last reaction of these is poorly con-

strained by experimental data and could potentially have a large impact on the production of ${}^7\text{Li}$ in BBN.

The rate estimates for $d+{}^7\text{Be}$ reactions in the commonly used Reaclib database [13] stem from an estimate by Parker [14], who multiplied cross-section data from Kavanagh [15] by an arbitrary factor of three and extrapolated to lower energies. An experiment performed at lower energy found a significantly reduced cross section in the BBN Gamow window compared to the Parker estimate [16]. Other works suggested resonant enhancement through a $5/2^+$ compound-nuclear state in ${}^9\text{B}$ [17, 18], an isospin-mirror to the 16.671 ($5/2^+$) state in ${}^9\text{Be}$. Candidates for such a state in ${}^9\text{B}$ were reported at 16.71 MeV [19] and at 16.80(10) MeV [20]. Without experimental knowledge of the partial decay widths, conclusions about resonant enhancements to the $d+{}^7\text{Be}$ reactions remained uncertain.

This paper describes an experiment measuring a complete excitation function for the $d+{}^7\text{Be} \rightarrow 2\alpha + p$ reaction at energies relevant for BBN. The experiment was performed at the John D. Fox accelerator laboratory of Florida State University, using the RESOLUT [21] radioactive beam facility to produce a beam of ${}^7\text{Be}$ of 19.7 MeV \pm 100 keV and an intensity around $5 \cdot 10^4 \text{s}^{-1}$, constituting 65% of the particles delivered to the experiment. The ${}^7\text{Be}$ beam particles were identified and selected off-line to $\geq 94\%$ purity through their time-of-flight signals measured with a thin-foil tracking detector located $\approx 3\text{m}$ upstream from the experiment. The beam composition was monitored by periodically inserting a compact detector into its path.

The beam of ${}^7\text{Be}$ was delivered to the ANASEN active-target detector [22], entering through a 8.9- μm thick Kapton window into a volume of pure deuterium gas at a pressure of 400 Torr, continuously losing energy in the gas until being stopped about 5 cm before the end of the detector. In this way, the excitation function of $d+{}^7\text{Be}$ reactions was simultaneously measured in one setting with

a single incident beam energy and with a common beam normalization. The beam axis was surrounded by an inner set of 24 position-sensitive proportional counters at 3.7 cm radius, surrounded by two “barrels” of 24 Micron Semiconductor “Super X3” silicon-strip detectors at a radius of 8.9 cm, while 4 Micron Semiconductor “QQQ3” detectors covered forward laboratory angles in an annular geometry. Each of the emitted light charged particles triggered a proportional-counter wire and a silicon-detector segment and was thus traced back to determine the reaction vertex location.

The detectors were calibrated with standard calibration sources in vacuum as well as by scattering of proton and helium beams off a thin gold foil within the deuterium gas volume. The position of the scattering target was varied along the beam axis to calibrate the position reconstruction in active gas-target mode. The energy-loss profiles in deuterium gas for protons, α and ${}^9\text{Be}$ particles were calibrated by injecting low-intensity accelerator beams into ANASEN and measuring the residual particle energies at various depths in the gas volume with an additional silicon detector. The data were fit and interpolated with energy-loss calculations in the program SRIM [23] and applied in the data analysis.

The light particles emerging from the reaction zone were identified through their characteristic energy losses in the proportional counter. The $d + {}^7\text{Be} \rightarrow 2\alpha + p$ reaction was clearly identified by requiring coincident detection of all 3 final particles. For each event, the reaction vertex was reconstructed from the trajectories of the two α -particles extrapolated to the beam axis. The beam energy at which the reaction occurred was determined from the reaction vertex and the calculated energy loss of the incident ${}^7\text{Be}$ to reach that point, which is called the “tracking method” (E_{track}). As a second, independent method labeled “sum method” (E_{sum}), the energies of the detected α and proton particles were summed and the fixed reaction Q-value subtracted, arriving at the reaction energy through energy conservation. Here, the detected particle energies were corrected for the energy loss on their way to the silicon detectors.

Fig. 1 compares the event analysis using both methods that show overall agreement. For each event, the reaction energies from both solutions were required to be consistent within ± 2 MeV, suppressing some background of mis-identified energies caused by scattering of light particles in ANASEN’s proportional-counter wires. In addition, consistency between the beam momentum and the total final-particle momentum vectors was required. The “sum-method” achieves a superior resolution of ≈ 400 keV in the laboratory and was used for the subsequent reconstruction of the excitation function.

The $d + {}^7\text{Be} \rightarrow 2\alpha + p$ reaction may proceed through intermediate states in ${}^8\text{Be}$ by the ${}^7\text{Be}(d, p){}^8\text{Be}(\alpha){}^4\text{He}$ reaction sequence, through intermediate states in ${}^5\text{Li}$ by the ${}^7\text{Be}(d, \alpha){}^5\text{Li}(p){}^4\text{He}$ sequence, or in a “democratic” three-

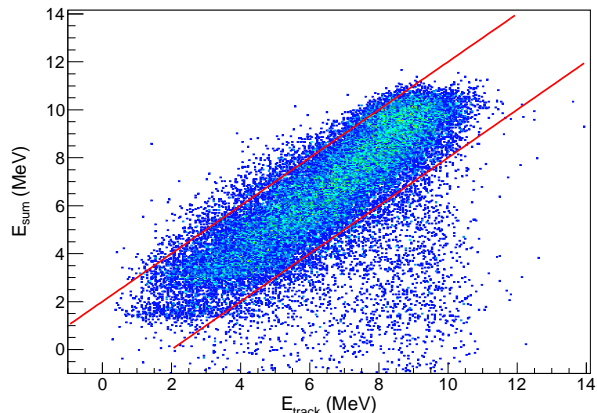


FIG. 1. Comparison of beam-particle energies reconstructed with two methods, the “sum method” (E_{sum}) and the “tracking method” (E_{track}), see text. Events between the two red lines were accepted for analysis.

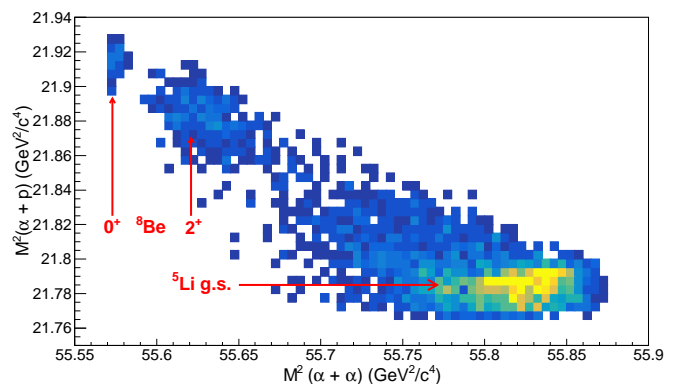


FIG. 2. Dalitz-plot analysis of $p + 2\alpha$ events at $E_{\text{cm}} = 1.15 \pm 0.20$ MeV, characterized according to the squared invariant masses of the $\alpha + \alpha$ and $\alpha + p$ systems. The lower of the two possible $\alpha_{1,2} + p$ invariant-mass values was selected.

particle decay of the ${}^9\text{B}$ compound system. Fig. 2 shows the distribution of events on a Dalitz-plot, where the x-axis corresponds to the $\alpha + \alpha$ invariant-mass squared and the y-axis to the $p + \alpha$ invariant-mass squared. Events are clearly grouped into those that pass through the ${}^8\text{Be}$ ground- and first-excited states, as well as events proceeding through the ${}^5\text{Li}$ ground state. The distribution of events at all energies is dominated by the ${}^7\text{Be}(d, \alpha){}^5\text{Li}(p){}^4\text{He}$ reaction, in contrast to the assumption of Angulo *et al.* [16], which analyzed cross sections assuming (d, p) kinematics.

The cross sections were determined from the number of events in each energy bin, the total number of incident ${}^7\text{Be}$ ions, the areal target density of each energy bin, and the simulated detection efficiency. The total number of incident ${}^7\text{Be}$ ions was determined from the integrated counts of the thin-foil tracking detector, corrected for beam purity ($\approx 65\%$) and the beam transmission into

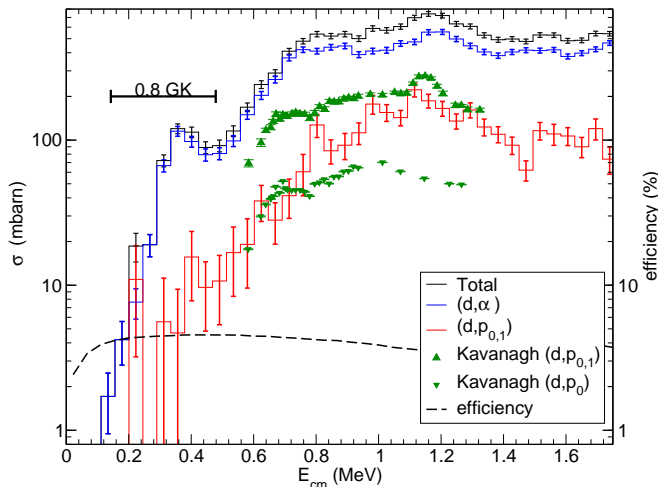


FIG. 3. Cross section as a function of the $d+{}^7\text{Be}$ center-of-mass energies, with statistical errors. The events are separated into (d, p) and (d, α) reactions, according to their location on the Dalitz-plot of Fig. 2. Shown for comparison are differential cross sections from Kavanagh [15], multiplied by 4π . The average detection-efficiency (dashed line) and the Gamow-window for $T = 0.8$ GK are also shown.

the ANASEN detector, ($\approx 29\%$). The overall normalization was estimated to be uncertain by 30%, the dominant uncertainty of the absolute cross sections. The combined efficiency for coincident detection of 3 particles was simulated with a Monte-Carlo model, taking into account the beam-energy profile, the three-particle reaction kinematics, the energy loss of particles in the target gas, the geometry and resolution of the detection systems as well as the number of events lost from scattering inside the detector volume. The three-particle detection efficiency covers the region of the Dalitz plot evenly, with the exception of ${}^7\text{Be}(d, p_0){}^8\text{Be}_{gs}$ events at the lowest reaction energies, for which there was low efficiency. Averaging over the phase-space, the energy dependence of efficiency is included in Fig. 3, which shows a consistent experimental sensitivity for $E_{c.m.} \geq 0.1$ MeV, covering the entire Gamow window for $T=0.8$ GK.

The resulting cross sections are displayed in Fig. 3, in total, as well as separated into the dominant (d, α) and the sum of the weaker $(d, p_0){}^8\text{Be}_{gs}$ and $(d, p_1){}^8\text{Be}_{2+}$ reaction sequences. Here, the efficiency correction was applied as a function of the events' Dalitz-plot coordinates. The cross sections exhibit features characteristic of resonant contributions, which include the dominant peak at $E_{c.m.} = 1.17$ -MeV resonance energy observed by Kavanagh [15] and other experiments [20, 24, 25]. The data also show a new resonance at $E_{c.m.} = 0.36(5)$ MeV, in the Gamow window of BBN. The proton-singles measurements of [15] likely contain an uncertain admixture of (d, α) contributions, which make a direct comparison ambiguous.

The data were analyzed using the multi-level R -matrix

code AZURE2 [26], separated into the (d, α) and the (d, p_1) channel populating the ${}^8\text{Be}$ first-excited state. The experimental angular distributions for the dominant (d, α) components at seven energies were simultaneously fit with the excitation functions to help constrain spin and parity of the resonances. For the (d, p_0) branch, which contributes about 15% to the total cross section, we also included the differential cross sections from Kavanagh [15] in place of our (d, p_0) data, which had inferior statistics. The resonance parameters to best fit the data are given in Table I, including two sub-threshold states (with parameters fixed to literature values) that were found to have some impact on the cross section. Some alternative spin-parity assignments resulted in comparable fits, but did not significantly alter the resulting reaction rates, which are well constrained by the data. The extracted strength for the $E_{c.m.} = 0.36(5)$ MeV ($5/2^+$) resonance is $\omega\gamma = 1.7(5)$ keV, with the uncertainty dominated by the overall cross-section normalization.

In Fig. 4 the experimental cross sections and the R -matrix fit using the parameters from Table I are represented through the astrophysical S-factor $S(E_{c.m.}) = \sigma(E_{c.m.}) \cdot E_{c.m.} \cdot \exp(2\pi\eta)$, with $\eta = q_1 q_2 / (\hbar v_{c.m.})$. The cross section in the Gamow-window of BBN is dominated by the $E_{c.m.} = 0.36(5)$ MeV ($5/2^+$) resonance. The figure also shows the two data points from Angulo *et al.*, the lower of which is consistent with our experiment's (d, p_1) cross section.

Figure 4 contains two representations of the R -matrix fit, one folding the data with the 100 keV $_{\text{FWHM}}$ experimental resolution (solid line) and one without folding (dashed line). The experimental-resolution curve shows an overall better fit, and a significant increase at low energies, similar to the experimental values. Comparison with the un-folded function shows that this increase is almost entirely explained by the limited experimental resolution. The 3 lowest-energy data points are each above the R -matrix fit by about 1σ , which could either be caused by a slight asymmetry in the experimental response, or additional, unknown sub-threshold states. The S-factor representation of the raw fit extrapolates to around 40 MeV \cdot barn towards the lowest energies, and was used to calculate the reaction rate. We found that fits including additional sub-threshold resonances or alternative experimental resolutions differed in the extracted reaction rates by less than 15% between temperatures of 0.05 and 0.5 GK.

The most important systematic uncertainty of the current measurement, in view of its astrophysical implications, lies in the calibration of $E_{c.m.}$, which is derived from detecting three particles with more than 16.5 MeV of total kinetic energy in the laboratory system. From the systematic uncertainties in the energy-loss corrections, the reconstructed reaction energies are uncertain by 200 keV in the laboratory, or 45 keV in the center of mass. To find the resulting uncertainties of the reaction rates, we ana-

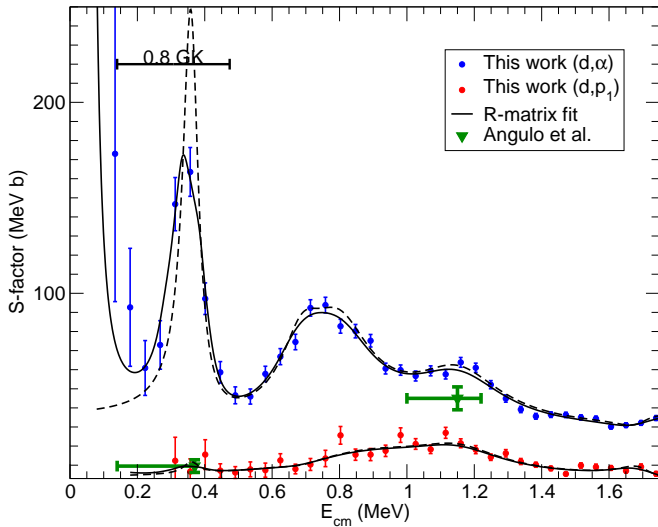


FIG. 4. S-factor representation of the experimental data for the (d, α) and the (d, p_1) channels. The continuous line represents the R -matrix fit including the $100 \text{ keV}_{\text{FWHM}}$ experimental resolution. The dashed line is an R -matrix calculation using the same resonance parameters without the experimental resolution included. Data points from Angulo *et al.* [16] are shown for comparison.

TABLE I. Properties of states in ${}^9\text{B}$ used in the R -matrix analysis. Excitation energies are in MeV, given with purely statistical uncertainties. Partial widths are in keV. Properties of the 2.8 and 14.7 MeV states are fixed in the analysis, taken from [27]. The 2.8 MeV state $\Gamma = 550 \text{ keV}$ is known to have a small Γ_α , for which we assume a 1% branch [28]. For the 14.7 MeV state we assume $\Gamma_\alpha = \Gamma_{p_1}$.

J^π	E_x	$E(d+{}^7\text{Be})_{c.m.}$	Γ_{p0}	Γ_{p1}	Γ_d	Γ_α
$(5/2^+)$	2.8	-	545	-	-	5
$(5/2^-)$	14.7	-	-	650	-	650
$(5/2^+)$	16.849 (5)	0.361 (5)	-	1	3.3	50
$(5/2^+)$	17.198 (9)	0.710 (9)	4	-	143	14
$(3/2^+)$	17.309 (21)	0.821 (21)	-	-	114	127
$(5/2^+)$	17.614 (28)	1.126 (28)	205	112	643	85
$(7/2^-)$	17.670 (11)	1.182 (11)	-	45	183	105
$(5/2^-)$	18.047 (32)	1.559 (32)	48	148	743	-
$(3/2^-)$	18.313 (83)	1.825 (83)	0.02	-	334	349
$(5/2^-)$	18.389 (17)	1.901 (17)	8	42	1600	1470
$(7/2^-)$	18.489 (7)	2.001 (7)	-	-	73	60
$(7/2^+)$	18.602 (88)	2.114 (88)	-	-	680	620

lyzed the rates derived from our excitation function after shifting it by $\Delta E = \pm 45 \text{ keV}$. The overall cross-section normalization uncertainty ($\pm 30\%$) was also included in the rate uncertainties.

The thermal reaction rates based on the R -matrix analysis (not including experimental resolution) are displayed in Fig. 5. The figure also compares rates calculated from previous experimental cross sections. The “Kavanagh” rates are based on an S -factor extrapolation of $33 \text{ MeV}\cdot\text{b}$ from the data of Kavanagh [15]. The rates following “An-

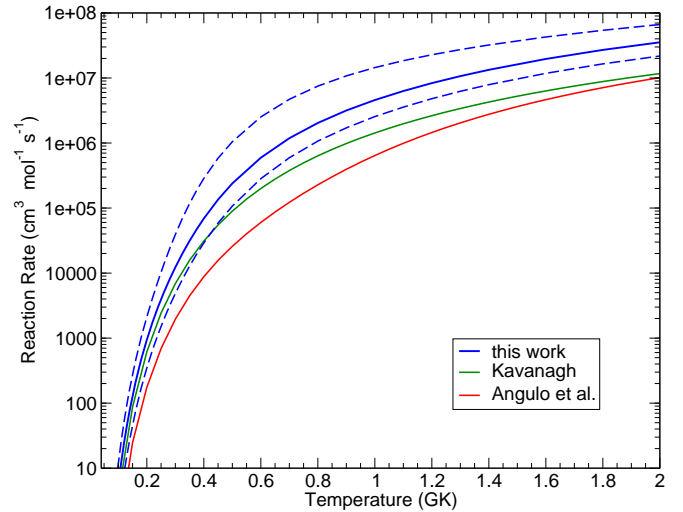


FIG. 5. Thermal reaction rates of $d+{}^7\text{Be}$ reactions as a function of temperature, calculated from R -matrix fit in this work, and in dashed line “high” and “low” values from systematic uncertainties. Rates calculated from Kavanagh [15] and Angulo *et al.* [16] are shown for comparison.

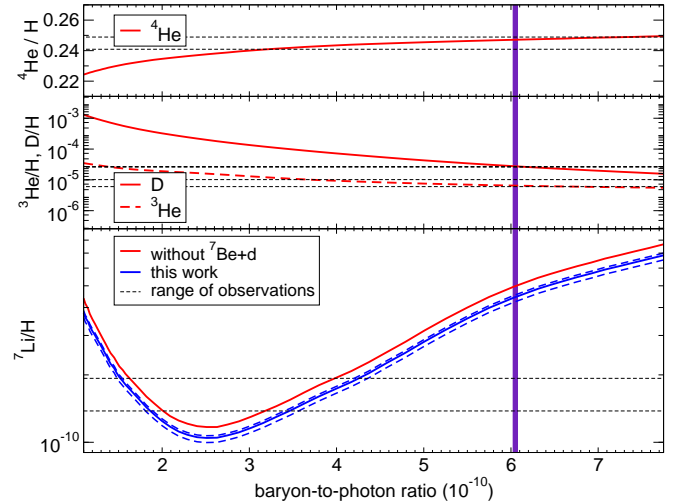


FIG. 6. BBN outcome for light isotopes as a function of baryon-to-photon ratio η . The relative ${}^7\text{Li}$ abundance was calculated using the experimental $d+{}^7\text{Be}$ reaction rate and its uncertainty range, which is compared to a BBN network without the $d+{}^7\text{Be}$ reaction. Horizontal dashed lines show range of observations [7].

gulo *et al.*” were calculated using the S -factor value of Ref. [16], combined with data from Kavanagh at higher energies.

These $d+{}^7\text{Be}$ reaction rates were used with other reaction rates taken from ReacliB [13, 29] to calculate BBN assuming a flat universe with $H_0 = 67.9 \text{ km/s/Mpc}$ [6]. The abundance of light elements as a function of the baryon-to-photon ratio η is shown in Fig. 6. The outcome for the “experimental rate” and its uncertainty range is

compared to that from a network with the $d+{}^7\text{Be}$ reaction removed. The abundances of other light isotopes are not measurably affected.

The baryon-to-photon ratio parameter η was determined by Planck to be $6.079(9) \cdot 10^{-10}$ [6], represented by the vertical band in Fig. 6. The reaction network *without* $d+{}^7\text{Be}$ reactions predicts BBN mass fractions of $({}^7\text{Li}/\text{H})_P = 5.05 - 5.08 \cdot 10^{-10}$, whereas our reaction rates predict $({}^7\text{Li}/\text{H})_P = 4.24 - 4.61 \cdot 10^{-10}$. The ${}^7\text{Li}$ mass-fraction values from our experiment are the lowest of the alternatives, but they do not solve the “primordial lithium problem”. It is interesting to note that the estimate by Parker [14], multiplying the Kavanagh data by an arbitrary factor three, predicts $({}^7\text{Li}/\text{H})_P \approx 4.51 \cdot 10^{-10}$, coincidentally in the middle of our range of values.

This experiment accurately measured $d+{}^7\text{Be}$ reactions in the Gamow-window of BBN for the first time. The majority of the reaction yield occurs in the (d, α) channel, which exhibits a $(5/2^+)$ resonance observed at $E_{cm} = 0.36(5)$ MeV with a resonance strength of $\omega\gamma = 1.7(5)$ keV. Additional experiments are needed to reduce the uncertainty in the resonance energy. If it is the same as the ${}^9\text{B}$ state observed at $E_{cm} = 0.31(1)$ MeV by Scholl *et al.* [20], the $({}^7\text{Li}/\text{H})_P$ mass fraction will fall at the lower end of this work’s range of uncertainties. Additional measurements with improved statistics at $E_{cm} < 0.2$ MeV would also be beneficial, but because of our experiment’s high sensitivity throughout most of the relevant Gamow window, it appears that the potential for significant additional resonant enhancement of the $d+{}^7\text{Be}$ reaction in BBN is closed.

This work was partially supported by the National Science Foundation, under grants PHY-1401574, PHY-1064819, PHY-1126345 and partially supported by the U.S. Department of Energy, Office of Science under grants DE-FG02-02ER41220 and DE-FG02-96ER40978 and DE-FG02-93ER40773. G.V.R. was also supported by the Welch Foundation (Grant No. A-1853). The authors thank R.J. deBoer for his helpful advice with the R -matrix analysis. I.W. would like to thank Donald Robson for suggesting this experiment over coffee.

* present address: Joint Institute for Nuclear Astrophysics, Michigan State University

- [1] R. H. Dicke, P. J. E. Peebles, P. G. Roll, and D. T. Wilkinson, *The Astrophysical Journal* **142**, 414 (1965).
- [2] A. A. Penzias and R. W. Wilson, *Astrophys. J.* **142**, 419 (1965).
- [3] R. V. Wagoner, W. A. Fowler, and F. Hoyle, *The Astrophysical Journal* **148**, 3 (1967).
- [4] G. F. Smoot, C. L. Bennett, A. Kogut, and et al., *The Astrophysical Journal Letters* **396**, L1 (1992).
- [5] G. Hinshaw, D. Larson, E. Komatsu, D. N. Spergel, C. L. Bennett, J. Dunkley, M. R. Nolta, M. Halpern, R. S. Hill, N. Odegard, L. Page, K. M. Smith, J. L. Weiland, B. Gold, N. Jarosik, A. Kogut, M. Limon, S. S. Meyer, G. S. Tucker, E. Wollack, and E. L. Wright, *The Astrophysical Journal Supplement Series* **208**, 19 (2013).
- [6] P. A. R. Ade *et al.* (Planck), *Astron. Astrophys.* **594**, A13 (2016), arXiv:1502.01589 [astro-ph.CO].
- [7] L. Sbordone, P. Bonifacio, E. Caffau, H. G. Ludwig, N. T. Behara, J. I. González Hernández, M. Steffen, R. Cayrel, B. Freytag, C. van’t Veer, P. Molaro, B. Plez, T. Sivarani, M. Spite, F. Spite, T. C. Beers, N. Christlieb, P. François, and V. Hill, *Astron. Astrophys.* **522**, A26 (2010).
- [8] B. D. Fields, *Annual Review of Nuclear and Particle Science* **61**, 47 (<https://doi.org/10.1146/annurev-nucl-102010-130445>).
- [9] R. H. Cyburt, B. D. Fields, K. A. Olive, and T.-H. Yeh, *Rev. Mod. Phys.* **88**, 015004 (2016).
- [10] A. Coc and E. Vangioni, *International Journal of Modern Physics E* **26**, 1741002 (2017).
- [11] A. Coc, P. Descouvemont, K. A. Olive, J.-P. Uzan, and E. Vangioni, *Phys. Rev. D* **86**, 043529 (2012).
- [12] R. T. Scherrer and R. J. Scherrer, *Phys. Rev. D* **96**, 083507 (2017).
- [13] R. H. Cyburt, A. M. Amthor, R. Ferguson, Z. Meisel, K. Smith, S. Warren, A. Heger, R. D. Hoffman, T. Rauscher, A. Sakharuk, H. Schatz, F. K. Thielemann, and M. Wiescher, *The Astrophysical Journal Supplement Series* **189**, 240 (2010).
- [14] P. D. Parker, *The Astrophysical Journal* **175**, 261 (1972).
- [15] R. Kavanagh, *Nuclear Physics* **18**, 492 (1960).
- [16] C. Angulo, E. Casarejos, M. Couder, P. Demaret, P. Leleux, F. Vanderbist, A. Coc, J. Kiener, V. Tatischeff, T. Davinson, A. S. Murphy, N. L. Achouri, N. A. Orr, D. Cortina-Gil, P. Figuera, B. R. Fulton, I. Mukha, and E. Vangioni, *The Astrophysical Journal Letters* **630**, L105 (2005).
- [17] R. H. Cyburt, B. D. Fields, K. A. Olive, and E. Skillman, *Astroparticle Physics* **23**, 313 (2005).
- [18] N. Chakraborty, B. D. Fields, and K. A. Olive, *Phys. Rev. D* **83**, 063006 (2011).
- [19] B. J. Pugh, *The (p,n) reaction on ${}^7\text{Be}$ and ${}^{17}\text{O}$ at 135 MeV*, Ph.D. thesis, Massachusetts Institute of Technology (1985), unpublished.
- [20] C. Scholl, Y. Fujita, T. Adachi, P. von Brentano, H. Fujita, M. Górska, H. Hashimoto, K. Hatanaka, H. Matushara, K. Nakanishi, T. Ohta, Y. Sakemi, Y. Shimbara, Y. Shimizu, Y. Tameshige, A. Tamii, M. Yosoi, and R. G. T. Zegers, *Phys. Rev. C* **84**, 014308 (2011).
- [21] I. Wiedenhöver, L. Baby, D. Santiago-Gonzalez, A. Rojas, J. Blackmon, G. Rogachev, J. Belarge, E. Koshchiy, A. Kuchera, L. Linhardt, J. Lai, K. Macon, M. Matos, and B. Rascol, *Proceedings of the 5th International Conference on “Fission and properties of neutron-rich nuclei” (ICFN5)*, 144 (2014).
- [22] E. Koshchiy, J. Blackmon, G. Rogachev, I. Wiedenhöver, L. Baby, P. Barber, D. Bardayan, J. Belarge, D. Caussyn, E. Johnson, K. Kemper, A. Kuchera, L. Linhardt, K. Macon, M. Mato, B. Rasco, and D. Santiago-Gonzalez, *Nuclear Instruments and Methods in Physics Research Section A: Accelerators, Spectrometers, Detectors and Associated Equipment* **650**, 100 (2011).
- [23] J. F. Ziegler, M. Ziegler, and J. Biersack, *Nuclear Instruments and Methods in Physics Research Section B: Beam Interactions with Matter* **199**, 100 (2005).
- [24] F. S. Dietrich, *Nuclear Physics* **69**, 49 (1965).
- [25] O. P. Gupta, A. Bond, and P. M. S. Lesser,

- Phys. Rev. C **18**, 1075 (1978).
- [26] R. E. Azuma, E. Uberseder, E. C. Simpson, C. R. Brune, H. Costantini, R. J. de Boer, J. Görres, M. Heil, P. J. LeBlanc, C. Ugalde, and M. Wiescher, Phys. Rev. C **81**, 045805 (2010).
- [27] D. Tilley, J. Kelley, J. Godwin, D. Mil-lener, J. Purcell, C. Sheu, and H. Weller, Nuclear Physics A **745**, 155 (2004).
- [28] D. H. Wilkinson, J. T. Sample, and D. E. Alburger, Phys. Rev. **146**, 662 (1966).
- [29] F.-K. Thielemann, M. Arnould, and J. W. Truran, in *Advances in Nuclear Astrophysics*, edited by E. Vangioni-Flam, J. Audouze, M. Casse, J.-P. Chieze, and J. Tran Thanh Van (1986) pp. 525–540.